Water Research X 28 (2025) 100380

Contents lists available at ScienceDirect

Water Research X

journal homepage: www.sciencedirect.com/journal/water-research-x

Irrigation systems as reservoirs of diverse and pathogenic *Pseudomonas syringae* strains endangering crop health

Marina Anteljević [a], Iva Rosić [a], Olja Medić [b,c], Tamara Ranković [b,c], Karolina Sunjog [d], Margareta Kračun-Kolarević [e], Stoimir Kolarević [e], Tanja Dreo [f], Aleksander Benčič [f,g], Tanja Berić [a,b,c], Slaviša Stanković [b,c], Ivan Nikolić [b,c,*]

[a] *University of Belgrade, Institute of Physics Belgrade, National Institute of the Republic of Serbia, Laboratory for Experimental Astrobiology, Pregrevica 118, Belgrade 11080, Serbia*
[b] *University of Belgrade, Faculty of Biology, Department of Microbiology, Studentski trg 16, Belgrade 11000, Serbia*
[c] *University of Belgrade, Faculty of Biology, Center for Biological Control and Plant Growth Promotion, Studentski trg 16, Belgrade 11000, Serbia*
[d] *University of Belgrade, Institute for Multidisciplinary Research, Kneza Višeslava 1, Belgrade 11000, Serbia*
[e] *University of Belgrade, Institute for Biological Research "Siniša Stanković", National Institute of the Republic of Serbia, Department of Hydroecology and Water Protection, Bulevar Despota Stefana 142, Belgrade 11060, Serbia*
[f] *National Institute of Biology, Department of Biotechnology and Systems Biology, Večna pot 121, Ljubljana 1000, Slovenia*
[g] *Jožef Stefan International Postgraduate School, Jamova 39, Ljubljana 1000, Slovenia*

ARTICLE INFO

Keywords:
Phytopathogen detection
Irrigation
qPCR
dPCR

ABSTRACT

Pseudomonas syringae (*Psy*) is a widely distributed bacterial species complex primarily recognized as a foliar pathogen but also inhabits diverse environments, including water habitats, where strains closely related to agricultural pathogens have been identified. The connection between *Psy*-caused epidemics and its potential presence in nearby irrigation systems remains underexplored. This study comprehensively examined the *Psy* complex in the Danube-Tisa-Danube Hydrosystem (DTD) in Serbia, assessing its abundance, phylogenetic diversity, and pathogenic potential. To reduce the reliance on the time-consuming steps of isolation and identification, we developed novel high-specific primers and probes for precise detection of strains belonging to phylogroup 2 within *Psy* complex. Our results demonstrated that dPCR, coupled with highly specific and sensitive primers, outperformed both traditional plating and qPCR in detecting the *Psy* complex and phylogroup 2 in irrigation waters, making *Psy* diagnostics more effective. Phylogenetic analysis indicated high strain diversity within the DTD, identifying phylogroups 1, 2, 7, 12, and 13 and haplotypes linked to strains previously encountered in epidemics on sugar beet in Serbia. Notably, 66.67% of the isolates from the DTD were capable of inducing disease. Phylogroup 2 isolates displayed a broad host range, suggesting that the dissemination of *Psy* from DTD through irrigation, poses a substantial threat to crop health and agricultural productivity.

Introduction

The condition of irrigation systems plays a vital role in supporting agricultural productivity and shaping the interactions between waterborne microorganisms and crops. Irrigation systems can act as pathways for the dispersal of plant pathogens, with repeated use of contaminated water sources posing significant risks to crop health and yield (Lamichhane and Bartoli, 2015). Within the broader water-food nexus, effective water resource management, including irrigation water quality and pathogen control, is essential for sustaining food production (Corona-Lopez et al., 2021; Salem et al., 2022). In this context, the Danube-Tisa-Danube Hydrosystem (DTD) in the northern part of Serbia, in Vojvodina Province, is important to its region. DTD is an artificial network of canals constructed for irrigation, drainage, and flood management (Blagojević et al., 2020). The total length of the main channel network is 930 km, which covers an area of around 12,000 km^2 (Blagojević et al., 2020). This hydrosystem is characterized by pronounced seasonal dynamics, influencing hydrological conditions such as water level and flow, temperature changes, water quality, biodiversity, and ecological processes. Recent initiatives aim to optimize its use for

* Corresponding author.
E-mail address: ivan.nikolic@bio.bg.ac.rs (I. Nikolić).

https://doi.org/10.1016/j.wroa.2025.100380
Received 22 April 2025; Received in revised form 9 July 2025; Accepted 14 July 2025
Available online 16 July 2025

irrigation across Vojvodina (FAO, 2021), a region renowned for its agricultural productivity and intensive crop cultivation. However, this area has also experienced numerous plant disease outbreaks (Ignjatov et al., 2017; Marković et al., 2022; Mitrović et al., 2015; Popović et al., 2013). Among the bacterial pathogens reported, members of the *Pseudomonas syringae* species complex (*Psy*) were most frequently associated with disease epidemics in crops, fruits, and vegetables in Vojvodina (Balaž et al., 2014; Iličić et al., 2021; Popović et al., 2015a, 2015b; Stojšin et al., 2015). *Psy* pathogens are recognized globally for their substantial impact on plant health and productivity (Morris et al., 2019).

Although primarily studied in agricultural context, recent research highlights *Psy*'s broader ecological significance, particularly in water systems such as rivers, lakes, groundwaters, and irrigation networks (Berge et al., 2023; Morris et al., 2010, 2023). *Psy* has also been detected in atmospheric environments like rain, snow, and clouds, where its ice nucleation proteins are thought to play an important role in cloud formation and precipitation, thereby influencing the global water cycle (de Araujo et al., 2019). This ability to persist and disperse in both agricultural and non-agricultural environments makes the diversity of strains found in non-agricultural habitats (e.g. fresh waters and irrigation channels) even more significant than those encountered in epidemic outbreaks (Berge et al., 2014; Morris et al., 2010).

Based on Multilocus Sequence Typing analysis, the complex is divided into 13 phylogroups, each representing a distinct evolutionary lineage (Berge et al., 2014). Among the reported epidemics detected in fields near the DTD canals, most were caused by phylogroup 2 (PG02), known for its wide host range, severe symptoms, high dispersal, and broad distribution (Morris et al., 2019, 2022). Given the proximity of numerous epidemics to the DTD, it is critical to investigate the *Psy* population in this canal network. In our previous study, *Psy* strains associated with earlier epidemics in cherry orchards were detected in the Danube River Basin of Serbia, which is linked to the DTD (Anteljević et al., 2023).

Various traditional and modern diagnostic techniques have been employed to detect *Psy*, including culture isolation, microscopy, PCR, and ELISA assay (Yang et al., 2023). Molecular techniques such as qPCR have proven highly effective in detecting and quantifying *Psy* in seeds (Chai et al., 2020), while both qPCR and dPCR (digital PCR) have been successfully employed for plant samples (Barrett-Manako et al., 2021). However, these methods require further improvement to achieve the sensitivity and specificity necessary for reliable detection in water samples (Kokkoris et al., 2021).

Our study aimed to provide a comprehensive assessment of *Psy* occurrence in DTD, an important water source for irrigation and agricultural production in a region where previous epidemics have affected sugar beet and vegetable crops. The main objectives of our study were to: (i) design specific primers and probes for the highly efficient detection of PG02 of the *Psy* complex, (ii) employ and compare traditional culture methods, qPCR, and dPCR assays to determine the abundance of the *Psy* complex and PG02 in the DTD, and (iii) investigate the pathogenic potential of isolated *Psy* strains and assess the risk for future *Psy* epidemics and crop health.

2. Materials and methods

2.1. Sampling sites and collection

Water samples were collected on April 20th and 21st, 2023, from eight locations at the DTD (Fig. 1 and Supplementary Material 1, Table S1). The DTD spans the northern region of the Republic of Serbia, located between the geographical coordinates 44° 51′ and 45° 52′ N latitude and 18° 51′ and 21° 17′ E longitude. The sampling sites were chosen based on prior reports of epidemics in Serbia linked to the *Psy* species complex (Supplementary Material 1, Table S2). Samples were taken approximately 3 m from the embankment at a depth of 30 cm below the water surface. In situ measurements of pH, temperature, conductivity, and dissolved oxygen (DO) were carried out using the portable multi-parameter instrument Multi 340i (WTW, Germany). Following the initial field measurements, water samples were stored at 4 °C, transported to the laboratory in cooling boxes, and processed immediately. Mass concentrations of ammonium (NH_4^+), nitrate (NO_3^-), nitrite (NO_2^-), and phosphate (PO_4^{3-}) were measured using colorimetric kits (FLUKA Analytical, Germany). These analyses were quantified using the WINLAB® DATA LINE PHOTOMETER (Dr. Lange, Germany). The

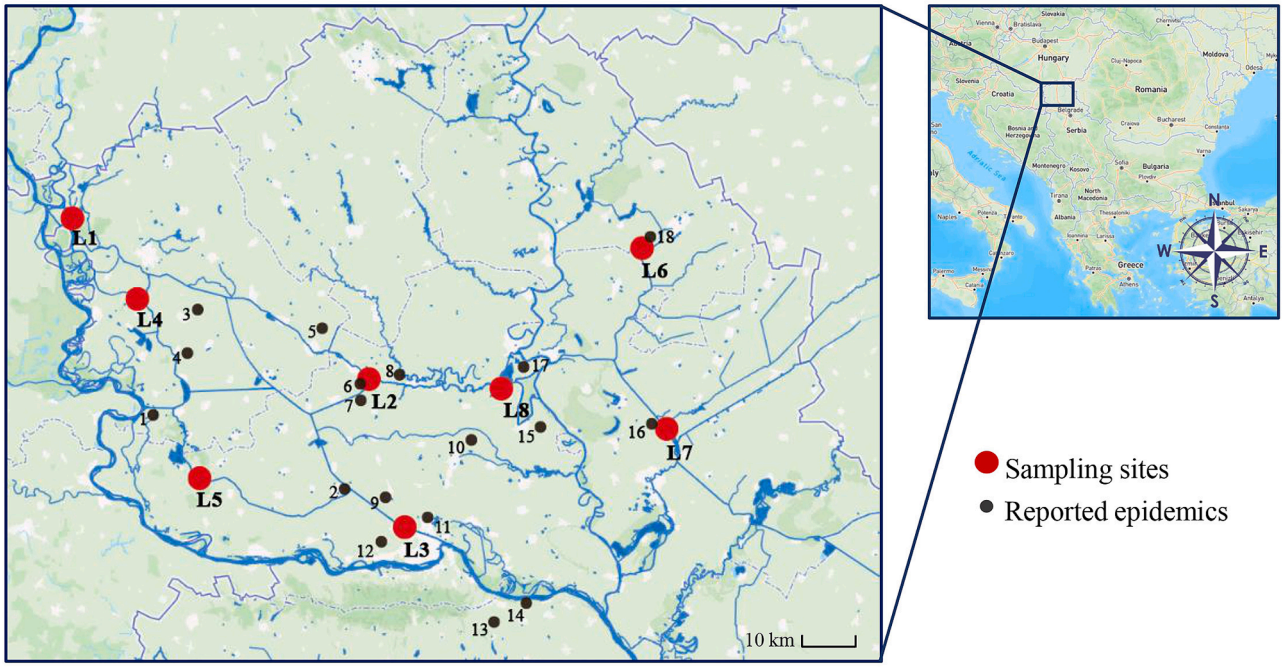

Fig. 1. Sampling locations on the Danube-Tisa-Danube Hydrosystem (red dots: L1 – Bezdan, L2 – Vrbas, L3 – Rumenka, L4 – Prigrevica, L5 – Bač, L6 – Kikinda, L7 – Jankov Most, L8 – Bačko Gradište) and nearby reported epidemics caused by P. syringae strains belonging to phylogroup 2 (black dots: 1 - epidemics on sweet cherry, 2 - oil pumpkin, 3–18 - sugar beet). Map created using Kepler.gl (https://kepler.gl).

photometric determination of NH_4^+, NO_3^-, NO_2^-, and PO_4^{3-} was based on specific chemical reactions that produce measurable color changes, with concentrations determined by comparison to calibration standards. All laboratory analyses were performed in accordance with standard protocols recommended by the manufacturers of the kits.

2.2. Sample processing – membrane filtration and microbiological analyses

One liter of water from each sampling site was filtered in two 500 mL steps using membrane filtration, with a new membrane filter used for each step. Mixed cellulose ester filters with a pore size of 0.45 μm and a diameter of 47 mm (Millipore, France) were employed. After filtration, one filter from each sample was used for total environmental DNA (eDNA) extraction using the ZymoBiomics DNA Miniprep Kit, with the eDNA stored at −20 °C for future analyses.

The second filter was immersed in 30 mL of sterile distilled water in an Erlenmeyer flask and subjected to agitation at 270 rpm for 15 min, followed by 1 min of sonication at 35 kHz in an ultrasonic bath. The 30 mL suspension was centrifuged at 2000 *g* for 20 min to concentrate the bacteria separated from the filter. The supernatant was discarded, and the bacterial pellet was resuspended in 1 mL of sterile distilled water, effectively concentrating the original sample 500-fold. This concentrated suspension was serially diluted and spread-plated onto King's medium B supplemented with cephalexin, boric acid, and cycloheximide (KBC), semiselective for *Pseudomonas* species (Mohan, 1987). The incubation step lasted for 5 days at room temperature.

Additionally, unfiltered water samples were used to quantify aerobic heterotrophic bacteria by dilution spread-plating on Nutrient Agar. The ratio of total heterotrophic bacteria (determined by pour-plating on Nutrient Agar) to oligotrophic bacteria (determined by pour-plating on 1:10 diluted Nutrient Agar) was also calculated after 4 days of incubation at room temperature.

The quantification of standard fecal indicator bacteria (SFIB), including *Escherichia coli*, total coliforms, and intestinal enterococci, was performed using the IDEXX Quanti-Tray 2000 system (IDEXX Laboratories, USA). The methodology is based on defined substrate technology (DST), which detects specific enzymatic activity related to each target organism. For *E. coli* and total coliforms, the Colilert-18 reagent was used, while Enterolert-E was used to identify and quantify intestinal enterococci. The substrate was added to 100 mL of the native or adequately diluted water sample. For total coliforms and *E. coli*, the Colilert-18 substrate is activated within 18 hours of incubation at 37 °C, where *E. coli* produces fluorescence and total coliforms induce a yellow color change. For intestinal enterococci, samples were incubated for at least 24 hours at a temperature of 44 °C. After incubation, the positive (color-changed or fluorescent) wells were counted to estimate the Most Probable Number (MPN) of SFIB in water.

2.3. PCR detection of Pseudomonas syringae complex

All *Pseudomonas* colonies from countable KBC plates (<300 colonies) were picked and subcultured to patch plates, where they were grown on fresh KBC medium for subsequent colony-PCR analysis. In the case of KBC plates with an uncountable number of colonies, only those resembling *Psy* were subcultured. We based our assessment on the description provided by Morris et al. (2022), who reported that *Psy* colonies are smooth with translucent, irregular edges, whereas some representatives exhibit a mucoid appearance but are not fully opaque. Colonies from the patch plates were subjected to a *P. syringae* species-specific PCR using primers Psy_F and Psy_R, designed by Guilbaud et al. (2016).

PCR reactions were carried out in a MiniAmp™ Thermal Cycler (Thermo Fisher Scientific, Waltham, Massachusetts, USA). The PCR mixture and conditions followed the protocol established by Guilbaud et al. (2016). Briefly, reactions were conducted in an 18 μL final volume, consisting of 10 μL of DreamTaq™ Green PCR Master Mix (2 ×), 6 μL of PCR water (Thermo Fisher Scientific, Waltham, Massachusetts, USA), and 0.55 μM of each *Psy*-specific primer. Bacterial cells from single colonies were collected using sterile pipette tips and directly transferred into PCR tubes containing the PCR mixture.

The thermal cycling conditions were as follows: an initial denaturation at 96 °C for 5 min, followed by 30 cycles of denaturation at 94 °C for 30 s, annealing at 61 °C for 30 s, extension at 72 °C for 30 s, and a final elongation step at 72 °C for 10 min.

PCR products were visualized on 1 % agarose gels containing ethidium bromide (0.4 μg/mL, SERVA, Germany) with a trans-illuminator (LKB, Transilluminator 2011 Microvue UV Light, Sweden). Electrophoresis was run in Tris-borate-EDTA (TBE) buffer (5.4 g Tris, 2.75 g boric acid, 4 mL of 0.5 M pH 8.0 EDTA, with dH_2O added to 1 L) at 90 V and 300 mA for 90 min. Colonies that tested positive for *Psy* (amplification of 144-bp specific fragment) were preserved in LB medium containing 20 % glycerol and stored at −80 °C. Total genomic DNA was extracted from the preserved isolates for further analysis using a modified CTAB protocol (Anteljević et al., 2023).

2.4. Phylogenetic and phenotypic analyses

To confirm the identity of *Psy* isolates from the DTD, a partial sequence of the *cts* housekeeping gene was amplified and sequenced using primers described by Morris et al. (2010). PCR amplification, purification, sequencing, and phylogenetic analysis followed the same methodology as in our previous study (Anteljević et al., 2023). The partial *cts* gene sequences (368 bp) were aligned with the Muscle program integrated into MEGA 11 software, which was also used to generate a phylogenetic tree with 1000 bootstrap replicates based on the neighbor-joining method to infer evolutionary relationships. Besides *Psy* reference strains, *P. graminis, P. rhizosphaerae, P. protegens*, and *P. aeruginosa* were included as out-groups. The tree was visualized using iTOL (Letunic and Bork, 2024) and rooted with *P. aeruginosa* PAO1. The partial *cts* gene sequences were deposited in NCBI under accession numbers PQ586931-PQ586972 (Supplementary Material 1, Table S1) and compared using the NCBI BLASTn tool to identify similarities with sequences available in the database, allowing us to investigate potential links to previous epidemics and distinguish haplotypes.

Phenotypic tests were performed to evaluate virulence-related traits of the *Psy* isolates, which were confirmed through *cts* gene analysis. These included the hypersensitive response assay on *N. benthamiana*, ice nucleation activity, pectinolytic activity, and motility assays (swimming and swarming). The preparation of bacterial suspensions and experimental procedures are in detail described in our previous work (Anteljević et al., 2023).

2.5. Host range

Pathogenicity tests were conducted on nine host plants (Table 1) to determine the host range. Plant species were chosen based on existing knowledge of previous infections in Serbia and the most commonly cultivated vegetables in the study area (FAO, 2022). We selected domestic cultivars of plants grown in Potgrond H substrate (Klasmann--Deilmann GmbH, Germany) within a greenhouse maintained at ambient temperatures. The virulence of *Psy* isolates from PG02, which tested positive in the hypersensitivity assay, was assessed. Bacterial suspensions for leaf inoculations were prepared from overnight cultures (grown in King's B medium at 30 °C, with agitation set at 180 rpm) by adjusting their optical density in fresh KB broth to $OD_{600} = 0.2$ (approximately 10^8 CFU/mL). Subsequently, suspensions were centrifugated at 13,000 g for 10 min and the precipitate was resuspended in sterile distilled water. One leaf per plant was inoculated with ~10 μL of a bacterial suspension at the abaxial side between two lateral nerves using a needleless syringae. Each isolate was tested in five replicates. Sterile distilled water was used as a negative control. Infected plants were incubated in a growth chamber with relative humidity maintained between 70–90 %, an

Table 1
Plant species and cultivars used for host range testing of Pseudomonas syringae isolates from the Danube-Tisa-Danube Hydrosystem.

Plant species	Cultivar	Age of plants at inoculation (months)	Source type
Beta vulgaris var. *saccharifera* (Sugar beet)	Heston	1	Seed
Solanum lycopersicum (Tomato)	Novosadski jabučar	1	Seed
Cucumis sativus (Cucumber)	Delikates	1	Seed
Pisum sativum (Pea)	Mali provansalac	1	Seed
Brassica oleracea var. *capitata* (Cabbage)	Futoški	1	Seed
Citrullus lanatus (Watermelon)	Slatka princeza	1	Seed
Capsicum annuum (Chili pepper)	Crveni ljuti	2	Seed
Petroselinum crispum (Parsley)	Lišćar	2	Seed
Allium cepa (Onion)	Kupusinski jabučar	1	Bulb

ambient temperature of 25 °C, and 12 h light/dark period. Plant-scoring was done 1, 3, 7, and 10 days after inoculation and the evaluation process was designed as an adjustment of the method used by Balthazar et al. (2022). Reactions were observed as three groups: no visible reaction, localized lesions at the inoculation zone and spreading lesions. In the case of spreading lesions, the percentage of leaf area exhibiting disease symptoms (necrosis and chlorosis around the inoculation zone) was measured by using ImageJ software (Schneider et al., 2012). Isolates were considered to have a pathogenic potential if at least three out of five replicate plants exhibited spreading lesions.

2.6. Design and validation of new qPCR tests

2.6.1. Design of qPCR tests for specific detection of P. syringae strains from phylogenetic group 2

Genomes of diverse *Pseudomonas* spp. strains were sourced from the NCBI GenBank database (Supplementary Material 2, Table S1). Employing DNA-DNA hybridization (DDH) values, the genomes were clustered using the Type Strain Genome Server (TYGS) web server (Meier-Kolthoff and Göker, 2019) for precise taxonomic classification, with the computational parameters set to default.

Genomes were categorized into "positive" and "negative" groups based on position in the phylogenetic tree. "Positive" included genomes of *Psy* strains from phylogenetic group 2 for which qPCR tests for specific detection were designed, while "negative" comprised all other strains. Five primer design analyses were conducted using different combinations of strains from both groups (Supplementary Material 2, Table S1). RUCS (Rapid Identification of PCR primers for Unique Core Sequences) webtool (Thomsen et al., 2017) was employed to identify unique core sequences (UCS) for the "positive" group. Computational parameters in RUCS webtool were set to default.

The primary RUCS output yielded a list of UCS for the "positive" genome group, organized based on their size. The top ten longest sequences were selected, and their associated genes were identified using the NCBI BLASTn tool. To ensure the exclusion of mobile genetic elements, unique core sequences not associated with such elements were considered for subsequent primer design.

These chosen UCS were then subjected to Primer Express v2.0 software (Applied Biosystems, USA) for the automated generation of qPCR primers and Taqman probes, with the default configuration of computational parameters. In instances where UCS identified by RUCS were too short for the design of the qPCR test, sequences were extended downstream. Using the CLC Main Workbench v 20.0.4 (QIAGEN) alignment tool, the augmented sequence underwent search for point mutations by comparing it to sequences of closely related strains determined through BLASTn.

The final selection of primers and probes adhered to the following criteria: the forward primer was based on the original unique core sequence, while the reverse primer and the probe were derived from the additional sequence (Supplementary Material 2, Table S2).

2.6.2. Genomic DNA isolation

All bacterial strains (Supplementary Material 2, Table S3) were cultivated on King's B agar medium before undergoing DNA isolation. The method employed for DNA isolation utilized thermal lysis in microtiter plates. A single colony of each bacterial strain was suspended in 100 µl of sterile Milli-Q water (Merck, USA). Subsequently, plates were heated at 100 °C for 5 min, then transferred to ice for 5 to 10 min. Afterward, the plates were briefly centrifugated and stored at −20 °C. The DNA extracted in this manner was used to assess the specificity of the primers in the qPCR method (Supplementary Fig. 1).

Genomic DNA from spiked samples (sugar beet phyllosphere homogenate combined with bacterial suspension) was extracted by the magnetic-bead-based QuickPick™ SML Plant DNA Kit (Bio-Nobile) as described by Pirc et al. (2009) with a slight modification (415 µL lysate for purification). The DNA was stored at ≤− 15 °C until analysis. The extracted DNA was utilized to evaluate the sensitivity of qPCR tests (Supplementary Fig. 1).

2.6.3. Setup of the qPCR tests

All four sets of primers and probe pairs were tested in 10 µL reactions, with the following composition: TaqMan 2 × Universal PCR Master Mix (Applied BiosystemsTM, USA) 5 µL, forward and reverse primer 0.9 µM each, probe 0.25 µM, Milli-Q water 2.80 µL, and 2 µL of DNA sample (from strains described Supplementary Material 2, Table S3). All reactions were performed in three technical repeats on 384-well plates, with each plate also including no-template control (NTC), a negative control of DNA isolation, and NIB Z 1237 (CFBP 1617) DNA as the positive control.

The qPCR amplifications were performed using the ViiA™ 7 Real-Time PCR System (Applied Biosystems, USA) under the following conditions: initial incubation for 2 min at 50 °C, followed by the activation of TaqMan polymerase for 10 min at 95 °C. Subsequently, 45 cycles were performed, consisting of denaturation for 15 s at 95 °C and hybridization/elongation for 1 min at 60 °C.

2.6.4. Validation of qPCR tests: analytical specificity

Given the well-documented diversity of the *Psy* complex, we decided to include strains from multiple sources to examine qPCR test specificity. In addition to 50 *Psy* strains isolated from the Danube River and DTD, we included 49 *P syringae* pv. *aptata* strains isolated from the sugar beet epidemics in Serbia (Nikolić et al., 2018), 16 *Psy* strains from various plant hosts, and 39 isolates from the sugar beet phyllosphere microbiota (Krstić Tomić et al., 2023) (Supplementary Material 2, Table S3). The specificity of the qPCR tests was evaluated by calculating true positives (TP), true negatives (TN), false positives (FP), and false negatives (FN) among the analyzed *Psy* and non-*Psy* strains. Obtained values were used to calculate the following parameters: analytical specificity - representing the ability of the method to identify true negatives among the total samples accurately [TN/(FP+TN)], percentage of false positives - indicating the proportion of samples falsely identified as positive [FP/total number of strains], percentage of false negatives - denoting the percentage of samples wrongly classified as negative [FN/total number of strains], inclusivity - measuring the method's capability to detect all strains expected to be positive [TP/(targets number)] and exclusivity - signifying the method's effectiveness in excluding samples that are supposed to be negative [TN/(non-targets number)].

2.6.5. Validation of qPCR tests: analytical sensitivity

A mixture of sugar beet DNA and bacterial DNA at different concentrations extracted from spiked samples was utilized to evaluate the sensitivity of the qPCR method (DNA extraction described in paragraph 2.6.2). Spiked samples were generated by combining 180 µl of sugar beet phyllosphere homogenate (10 g of leaf ground using a mortar and pestle in 5 mL 1 × PBS buffer (1.08 g Na_2HPO_4, 0.4 g $NaH_2PO_4 \times 2H_2O$, 8 g NaCl, 1 L distilled water, pH 7.2)) with 20 µl of bacterial suspension to obtain concentrations ranging from 10^8 cells/mL to 10 cells/mL. Bacterial suspensions for three *P. syringae* pv. *aptata* (*Ptt*) strains (P21, P16, and NIB Z 1237 (CFBP 1617)) were prepared by resuspending colonies in 5 mL of 10 mM PBS buffer with 10 % glycerol (v/v). The concentrations of the bacterial suspensions were determined turbidimetrically using a densitometer (DEN-1B; BioSan, Riga, Latvia). The sensitivity of the method was determined by comparing Ct values across concentrations of bacteria ranging from 10^8 cells/mL to 10 cells/mL for three *Ptt* strains. Additionally, logarithmic concentrations with their corresponding Ct values were graphically connected. A linear trendline equation was calculated based on this relationship. The qPCR tests' amplification efficiency (E) was then calculated using the standard curve slope. The efficiency was determined using the formula: $E = (10^{(-1/\text{slope})} - 1) \times 100$ (Supplementary Fig. 1).

2.7. Detection and quantification of Pseudomonas syringae complex and phylogroup 2 using qPCR

eDNA samples from eight sites within the DTD (Fig. 1) were analyzed using qPCR testing to detect *Psy* complex and PG02. For the reactions targeting the *Psy* complex, the primers Psy_F and Psy_R, originally designed by Guilbaud et al. (2016), were used, along with a probe (5′-FAM-TAAAGTGATCGACAAGGGCGCTGA-BHQ_1–3′) designed using the PrimerQuest™ Tool (Integrated DNA Technologies, USA). To optimize the reaction mix, we evaluated four different formulations with varying concentrations of primers and probes on strain *Ptt* P21 as a positive control (Supplementary material 3, Table S1). The final reactions were conducted on eDNA samples using a mix containing 5 µL of TaqMan 2 × Universal PCR Master Mix (Applied Biosystems™, USA), 5 µM of both forward and reverse primers, and 1.6 µM of the probe. Two concentrations of eDNA samples were tested, at 1 ng/µL and 2 ng/µL, with Milli-Q water added to achieve a final reaction volume of 10 µL. All reactions were conducted in triplicate. To assess the method's sensitivity, qPCR was conducted on serial dilutions of positive control *Ptt* P21 DNA at concentrations of 0.5, 1, 1.5, and 2 ng/µL. The resulting Ct values were plotted against the logarithmic DNA concentrations to generate a standard curve, and amplification efficiency was calculated (paragraph 2.6.5).

For the detection of PG02, the Psa_AvrE1 primer pair and probe were used (Supplementary Material 3, Table S2) with a qPCR reaction mix prepared as previously described and 2 ng/µL of eDNA sample (paragraph 2.5.3).

The qPCR reactions were executed using the ViiA™ 7 Real-Time PCR System (Applied Biosystems, USA). As described in paragraph 2.6.3, the thermal cycling conditions were identical for both target groups. qPCR was used to quantify the target DNA in the sample and to calculate the abundance of the *Psy* complex and PG02 in the DTD, as target sequences are present in one copy per genome. Copies per microliter of reaction were determined by interpolating Ct values from a standard curve. These values were then adjusted based on the total DNA extracted from the water sample and the water sample volume, allowing the final results to be expressed as cp/L (copies per liter of water).

2.8. Digital PCR (dPCR) for detection and quantification of Pseudomonas syringae complex and phylogroup 2

dPCR was performed on eight eDNA samples from sites within the DTD (Fig. 1) using a QX200 Droplet Digital System (Bio-Rad) according to the manufacturer's instructions. Each dPCR reaction mixture (total of 20 µL) consisted of 10 µL of 2 × digital PCR Supermix for Probes, 0.9 µM forward and reverse primers, 0.25 µM probe (sequences for both assays are provided in Supplementary Material 3, Table S2), and 2 µL of template DNA (resulting in a final concentration of 1 ng/µL in the reaction). Droplets were generated using the QX200 Droplet Generator, and PCR amplification was conducted on a Bio-Rad T100 thermal cycler under the following conditions: initial denaturation at 95 °C for 10 min, followed by 40 cycles of 94 °C for 30 s and 59.3 °C for 60 s (with a ramp rate of 2 °C/s), and a final extension at 98 °C for 10 min. Droplets were analyzed using the QX200 Droplet Reader, and only samples with a minimum of 10,000 droplets generated were considered for analysis. Fluorescence data were analyzed using QX Manager Software (version 2.1), with the threshold for positive droplets set manually based on the fluorescence amplitude of no-template controls and positive controls (DNA extract of strain BFD143). The Limit of Quantification (LOQ) was determined by analyzing serial dilutions of the BFD143 DNA extract, where LOQ was set as the lowest concentration, yielding a coefficient of variation (CV) $\leq$25 % across five replicates (Supplementary Material 4, Figs. S1 and S2). The Limit of Blank (LOB) was calculated using the mean value of blank samples (bm) and their standard deviation (stdev), following the formula: $\mathbf{LOB = bm + 1.65 \times stdev}$ (Clinical and Laboratory Standards Institute 2004). Samples that did not meet the LOQ thresholds were assessed qualitatively as either presence or absence of the target DNA. A sample was considered positive if its value exceeded the LOB threshold.

The number of target copies per microliter in the dPCR reactions was used to quantify the *Psy* complex and PG02. These values were then adjusted based on the total DNA extracted from the water sample and the sample volume, allowing the final results to be expressed as cp/L.

2.9. Statistical analyses

Statistical analysis of the dPCR data was conducted using GraphPad Prism (version 8.4.3). Group differences were assessed by one-way ANOVA with Tukey's HSD post hoc test, with significant differences marked at $p < 0.05$.

To assess the agreement between the *cts*-based identification and dPCR methods for quantifying *Psy* complex abundance in the DTD, a Bland-Altman analysis was performed on log-transformed data using GraphPad Prism (version 8.4.3). The percentage difference between the two methods was calculated using the formula:

$$\textit{Percentage difference} = 100 \times \frac{(A - B)}{\textit{Average of A and B}}$$

Where A represents the quantification of *Psy* abundance by the *cts*-based identification method, B represents the quantification by dPCR, and the average is the mean of the two methods ($\frac{A+B}{2}$). The resulting percentage differences were then plotted against the average values to assess the agreement between the two methods.

For the host range test, statistical analyses were performed using RStudio software (version 2024.09.0, R version 4.3.2) with the stats (R Core Team, 2024) and dunn.test (Dinno, 2017) packages, while the ggplot2 (Wickham, 2016) package was used for data visualization.

The normality of the data was assessed using the Shapiro-Wilk test, conducted on both non-transformed and log-transformed datasets. Since the data did not follow a normal distribution, non-parametric tests were applied. The Kruskal-Wallis test was used to compare symptom severity among groups based on bacterial strains, host plants, and sampling days. To evaluate the differences in symptom severity caused by various bacterial isolates on the same plant host across different days, Dunn's test was performed as a post-hoc analysis following the Kruskal-Wallis test. This test compares all possible pairs of bacterial isolates within each host and day combination to identify statistically significant differences in symptom severity. The resulting p-values were adjusted for

multiple comparisons using the Bonferroni correction to control for Type I error. The most significant differences were extracted for each day-host combination and visualized to highlight the key findings of the analysis. Additionally, a K-means clustering analysis was performed to group bacterial strains based on their overall aggressiveness in causing symptoms across different host plants. Clusters were visualized to observe similarities between strains.

3. Results

3.1. Water quality of the DTD hydrosystem shows spatial variability

Measurements of physicochemical and microbiological parameters were conducted on eight sampling sites of the DTD: L1 – Bezdan, L2 – Vrbas, L3 – Rumenka, L4 – Prigrevica, L5 – Bač, L6 – Kikinda, L7 – Jankov Most, L8 – Bačko Gradište (Fig. 1). Water temperature ranged from 13.3 °C at site L7 to 17.1 °C at site L5, typical for spring conditions (Supplementary Material 1, Table S3). Conductivity, which reflects ion concentration, was highest at L3 (608 µS/cm) and lowest at L7 (422 µS/cm). Oxygen levels showed considerable variation, with the highest concentration measured at L2 (19.4 mg/L) and the lowest at L6 (5.5 mg/L). The pH levels indicated slightly alkaline conditions across the sites. Ammonium, nitrate, and phosphate concentrations were higher at L6 and L7, suggesting increased nutrient inputs at these sites.

In terms of microbiological water quality, the sites L6 and L7 displayed the most concerning results, with excessive counts of total coliforms, intestinal enterococci, and aerobic heterotrophs, indicating significant fecal and organic pollution (Supplementary Material 1, Table S3). At site L1, these groups had relatively low total counts, indicating minimal contamination. The oligotroph-to-heterotroph ratio was highest at L2 (25.54), suggesting lower nutrient availability compared to other sites. In contrast, L1 (0.58), L6 (0.86), and L5 (0.76) had lower ratios, indicating higher nutrient availability and greater heterotrophic activity, often linked to pollution.

Among the eight sites where physicochemical and microbiological parameters were assessed, only L4 and L8 met the criteria for indication of good to moderate ecological potential (Class II-III), according to the standards applied to artificial water bodies in Serbia (Official Gazette of the Republic of Serbia No.74/2011 2011). The other six sites would thus classify within moderate to poor ecological potential (Class III-IV) based on parameters that exceeded optimal limits.

3.2. Isolation and cts gene-based identification revealed high abundances of Pseudomonas syringae in the Danube-Tisa-Danube Hydrosystem

To detect and isolate representatives of *Psy* from samples collected at eight different sites within the DTD canal network, a total of 651 bacterial colonies isolated on semi-selective KBC media were screened using species-specific PCR primers targeting the *Psy* complex (Supplementary Material 1, Table S1). Of the 651 colonies, 68 (10.45 %) showed

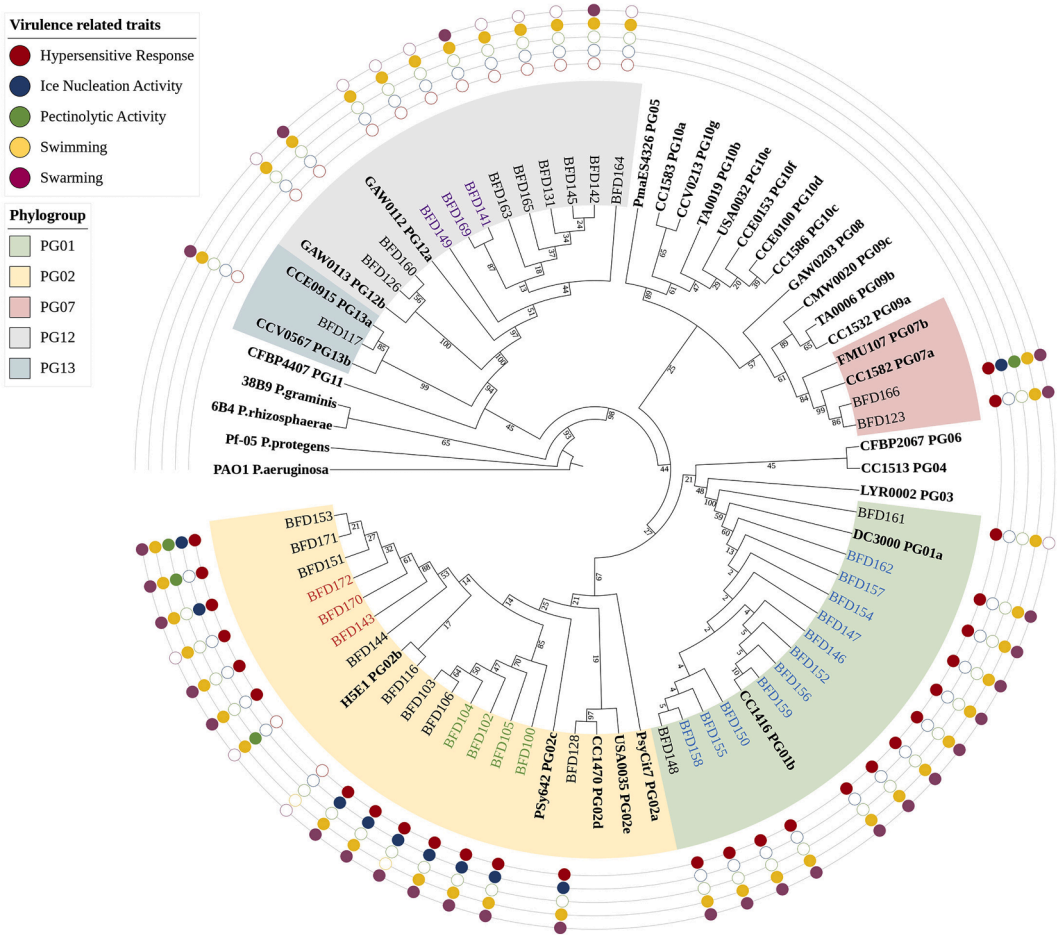

Fig. 2. The phylogenetic tree of *Pseudomonas syringae* isolates constructed based on the partial sequence of the *cts* gene. A phylogenetic relationship between 42 *Psy* isolates from the Danube-Tisa-Danube Hydrosystem (BFD labeled isolates), reference strains representing 13 phylogroups, and strains used as out-groups (in bold) is shown. The tree was generated by the neighbor-joining method. Bootstrap values (expressed as a percentage of 1000 replications) are shown at branch nodes. The presence (colored circles) or absence (empty circles) of tested phenotypic traits is displayed next to each isolate. Isolate codes labeled with the same color (red, green, blue, and purple) share the identical *cts* sequence.

successful amplification of a specific 144-bp fragment, and those were considered putative *Psy*. The identity of these isolates was further validated by DNA sequencing of the partial *cts* gene, coding for citrate-synthase, a key enzyme in regulating energy generation of mitochondrial respiration (Cheng et al., 2009). Among the initial 68 isolates, 42 (68 %) were finally confirmed as *Psy* and preserved in a strain collection (Supplementary Material 1, Table S1).

The abundance of the *Psy* complex at each site varied significantly in a range of 10^4– 10^7 CFU/L (Supplementary Material 1, Table S1). Site L5 displayed the highest *Psy* abundance, reaching 1.9×10^7 CFU/L, while the lowest confirmed abundance was at L1 with 6×10^4 CFU/L. At L6, none of the colonies were confirmed as *Psy* by *cts* sequencing, so this site was excluded from abundance calculations.

Phylogenetic analysis of the 42 confirmed *Psy* isolates, based on the *cts* gene (368 bp), revealed the presence of five distinct phylogroups within the DTD (Fig. 2): PG01 (30.9 %), PG02 (35.7 %), PG07 (4.8 %), PG12 (26.2 %), and PG13 (2.4 %). Phylogroup 2 was the most widely distributed, being detected at four different sites. The abundance of PG02 was the highest at site L5 (6×10^6 CFU/L) (Supplementary material 1, Table S4). Notably, L5 exhibited the highest diversity, with four distinct phylogroups identified at this site. We could observe the dependence of the phylogroup distribution on the sampling point. At the rest of the sites, the presence of only one or two phylogroups was confirmed (Supplementary Material 1, Table S1).

Further comparisons of the isolates' *cts* sequences with publicly available sequences in the NCBI database revealed 25 distinct haplotypes among the 42 isolates, some of which showed 100 % identity in nucleotide sequence to previously described strains (Supplementary Material 1, Table S5). In PG02, a group of isolates (BFD143, BFD170, and BFD172) shared identical *cts* sequences with the DD.1 haplotype described by Morris et al. (2023), which has been reported as a widespread haplotype in river water, possessing a highly virulent phenotype. It matches many plant pathogenic strains, including *P. syringae* pv. *aptata* from earlier epidemics on sugar beet in Serbia. Similarly, another haplotype within PG02 isolates (BFD100, BFD102, BFD104, and BFD105) corresponded to strains previously isolated from diverse environments such as freshwater in France (Berge et al., 2014), snow in Switzerland, and stone fruits in Poland.

In phylogroup 1, a larger group of isolates (BFD146, BFD147, BFD150, BFD152, BFD154, BFD155, BFD156, BFD157, BFD158, BFD159, and BFD162) displayed identical *cts* sequences. These sequences matched the reference strain *P. syringae* CMO0017, isolated from rainwater in France, and a strain isolated from kiwi fruit plants in Spain. Additionally, another set of isolates from PG12 (BFD141, BFD149, and BFD169) shared 100 % sequence identity with the reference strain *P. syringae* GAW0112, isolated from an irrigation canal network in France. Considering these concurrences, we observed that half of the isolates from our collection (21) belong to some of the haplotypes previously detected in river or rainwater.

3.3. *Pseudomonas syringae isolates from the Danube-Tisa-Danube Hydrosystem exhibited virulent traits important for pathogenic lifestyle*

The examination of hypersensitive response (HR), ice nucleation activity (INA), pectinolytic activity (PA), and motility capabilities in the isolates from our collection provided insight into their virulence potential (Fig. 2). A hypersensitive response was induced by 28 isolates (66.67 % of the collection), indicating the pathogenic potential of these strains. The isolates that caused the necrotic zones in the inoculated leaf areas belonged to phylogroups 1 (46.4 %), 2 (46.4 %), and 7 (7.2 %). In contrast, isolates from phylogroups 12 and 13 did not induce a hypersensitive response, consistent with current findings regarding these groups (Berge et al., 2014; Morris et al., 2022). Regarding INA, only ten isolates (23.8 %) promoted ice formation at temperatures ranging from −2 °C to −10 °C. One ice-nucleating isolate belonged to PG07, and the others belonged to PG02. The highest temperature at which ice formation was observed was− 4 °C, noted in isolates BFD128 and BFD153. INA was only observed in isolates that induced HR, suggesting an association between these two traits. The pectinolytic activity was detected in four isolates (9.5 %), while motility was a much more widespread trait, with swimming observed in 40 isolates (95.2 % of the collection) and swarming in 30 isolates (71.4 %). Isolates BFD104 and BFD116 from PG02 were the only ones lacking swimming ability, while swarming was predominantly absent in isolates from PG12.

Among the *Psy* isolates from the DTD, BFD153 (PG02) and BFD166 (PG07) were the only strains to test positive for all virulence traits, while BFD116 (PG02) was the only isolate negative for all traits. The most common trait combination, observed in 15 isolates from phylogroups 1 and 2, included HR, swimming, and swarming. Many non-swarming isolates could not induce HR, indicating that swarming ability may be a critical factor for disease development. Considering the observed virulence traits of the *Psy* population representatives from the DTD, we could also conclude that certain strains could negatively affect nearby crops through irrigation practices, posing a risk to agricultural productivity.

3.4. *Phylogroup 2 representatives of Psy complex induced severe symptoms in a wide range of host plant tested*

PG02 was the most commonly identified as a causative agent of diseases in crops in the region within the DTD canal network, among other phylogroups. To assess the epidemiological risk of the isolated *Psy* PG02 strains, we conducted pathogenicity tests on economically important vegetables widely cultivated for human consumption, as well as on sugar beet, an industrial crop that was severely affected by *Ptt* outbreaks in Vojvodina Province over the past decade (Nikolić et al., 2018). Out of 15 representatives of PG02 isolated from the DTD, 13 isolates that triggered a hypersensitive reaction in *Nicotiana benthamiana* (BFD128 from clade 2d, and the other twelve from clade 2b) were tested for pathogenicity on nine different plant species. Lesion spreading in some cases was already evident by day 3. Generally, the isolates exhibited a broad host range, with at least five plant species developing visible symptoms. Isolates BFD128, BFD151, BFD171, and BFD172 were the most virulent, inducing symptoms across all plant species tested. In contrast, isolate BFD102 displayed the narrowest host range (Fig. 3a). Chili pepper and watermelon exhibited the highest resistance, as more than half of the tested isolates were unable to induce disease symptoms in these hosts.

Statistically significant differences in symptom severity across plant hosts depending on the bacterial strain were confirmed (Chi-square = 1358.8, $p = 1.11 \times 10^{-118}$, df = 350), with the most significant findings attributed to BFD100 and BFD128 isolate combination. Notably, isolate BFD128 consistently induced more severe symptoms compared to BFD100, particularly on tomato ($Z = -5.88181$), sugar beet ($Z = -4.06315$), and chili pepper ($Z = -4.04011$). The pronounced aggressiveness of BFD128 highlights its high virulence relative to the other tested strains (Fig. 3b).

Based on average symptom severity, isolates were grouped into three clusters through K-means clustering: Cluster 1 (high severity, 59.08–100 % symptom severity), Cluster 2 (low severity, 0–20.06 %), and Cluster 3 (moderate severity, 21.49–36.66 %) (Fig. 3c). On the third day post-inoculation, the majority of isolates were classified within the low-severity cluster. By day 7, a more significant number of plant hosts exhibited moderate to high-severity symptoms, with isolate BFD128 notably causing severe symptoms in cabbage, tomato, and chili pepper. On day 10, the incidence of high-severity symptoms increased further. Notably, chili pepper and watermelon remained the only hosts without high-severity symptoms, underscoring their resilience. Observations of symptom severity 10 days post-inoculation indicate the presence of two groups of isolates differentiated by their aggressiveness. A less aggressive group, consisting of strains BFD100, BFD102, BFD103, BFD104, BFD105, and BFD106, was characterized by only a few instances of

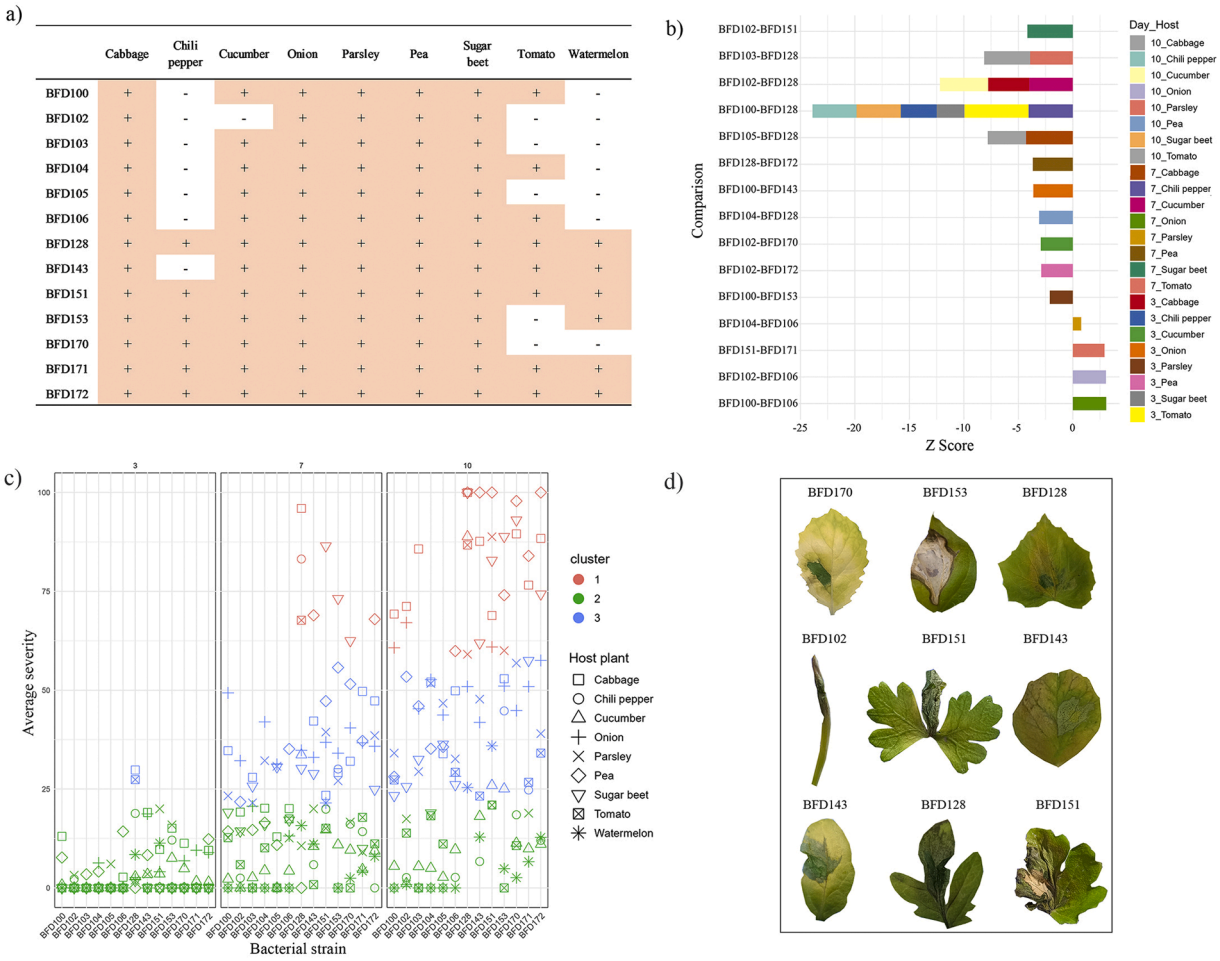

Fig. 3. Analysis of *Pseudomonas syringae* phylogroup 2 isolates from the Danube-Tisa-Danube Hydrosystem in host range tests. a) A table displaying the presence (+) or absence (−) of disease symptoms on plant hosts infected with phylogroup 2 isolates, observed 10 days post-inoculation. b) Dunn's post hoc test results, showing the most statistically significant differences in symptom severity caused by isolate pairs for each host and day combination. Higher absolute Z-scores indicate more substantial evidence of significant differences. c) K-means clustering results categorizing isolates across days based on symptom severity percentages: Cluster 1 (high severity, 59.08–100 %), Cluster 2 (low severity, 0–20.06 %), and Cluster 3 (moderate severity, 21.49–36.66 %). d) Representative leaf specimens of each host showing symptoms caused by the most aggressive isolate on day 10 (layout of plant species tested: Upper row – cabbage, chili pepper, cucumber; middle row – onion, parsley, pea; bottom row – sugar beet, tomato, watermelon).

highly severe symptoms. Conversely, the more aggressive group, including BFD143, BFD151, BFD153, BFD170, BFD171, BFD172, and BFD128, induced highly severe symptoms in a larger number of tested hosts, underscoring the threat posed by their presence in the DTD (Fig. 3d).

3.5. *Designed qPCR tests exhibit high specificity for the detection of phylogroup 2 within Pseudomonas syringae complex*

Given the ubiquity and pathogenicity of PG02 representatives of the *Psy* complex, we aimed to develop specific and sensitive qPCR tests for their detection. Four qPCR primer pairs and corresponding probes were designed based on the genes *avrE1* (encoding a type III secretion system effector), *cstA* (carbon starvation protein), *pleD* (diguanylate cyclase), and *avrE2* (another type III secretion system effector) (Supplementary Material 2, Table S2). The specificity of all four sets of primers and probes was primarily evaluated for detecting PG02. All tests were conducted on 154 bacterial strains, representing various phylogroups of the *Psy* complex and other genera (Supplementary Material 2, Table S4).

The Psy_AvrE1 primer and probe set proved to be the most effective for detecting representatives of PG02, achieving 100 % analytical specificity by correctly identifying all 74 tested strains from PG02, with no false positives or negatives among the additional 80 non-target strains tested (Supplementary Material 2, Table S5). This suggests that Psy_AvrE1 could be a reliable tool for detecting PG02 strains.

Sensitivity tests using spiked samples with varying concentrations of *Psy* (PG02) strains revealed that the Psy_AvrE1 primer and probe set consistently detected bacteria across all replicates down to 5×10^3 cells/mL, confirming its high sensitivity (Supplementary Material 2, Tables S6, S7, S8, and Fig. S1). The qPCR assay using the Psy_AvrE1 primer set consistently detected bacterial DNA, demonstrating its robustness in complex sample matrices containing plant-derived DNA.

3.6. *qPCR detection of Pseudomonas syringae complex and phylogroup 2 in the Danube-Tisa-Danube Hydrosystem was successful across samples tested from all sites*

To detect and quantify the *Psy* complex and PG02, we performed qPCR on eDNA samples collected from all eight sites within the DTD. For the *Psy* complex, we employed the set of previously designed *Psy* primers (Guilbaud et al., 2016) and the PsyP TaqMan probe we designed to improve specificity. MIX3 was selected due to its consistent performance and reliable detection in optimization assays with positive controls at an eDNA concentration of 2 ng/μL, with a reaction efficiency of 114 %, which falls within the acceptable range for qPCR assay reliability (Supplementary Material 3, Table S1). The target DNA was detected in

each sampling site, though not consistently across all replicates. Due to variability in results, precise quantitative interpretation remains limited. The exception is the site L3 with the consistent Ct values across replicates, yielding an estimated population of 1.42×10^5 cp/L (Supplementary Material 5, Table S1).

The Psy_AvrE1 primers and probe set were employed to detect PG02 in the DTD system at the tested sites. The qPCR assay using the Psy_AvrE1 primer pair proved effective in detecting the presence of PG02 at each site, making it suitable for initial screening of their presence. However, its quantification potential was limited in most cases, as the assays with eDNA samples introduced obstacles and variations. The calculated population densities for sites L4 and L8 were on the order of 10^4 cp/L, with both sites consistently testing positive across replicates and exhibiting minimal standard deviations (Supplementary Material 5, Table S2).

3.7. dPCR outperforms the cultivation method in both the detection and quantification of the Pseudomonas syringae complex in the Danube-Tisa-Danube Hydrosystem

We applied the dPCR method to quantify the *Psy* population at eight sites within the DTD and to assess the abundance of PG02, following qPCR tests performed with the *Psy* primers described by Guilbaud et al. (2016) and the designed probe, as well as the Psa_AvrE1 primer and probe set for PG02. This transition to dPCR was made to achieve a more precise quantification (Fig. 4).

The target DNA concentration was above the verified limit of quantification (LOQ) for the *Psy* assay at each site (Supplementary Material 4, Fig. S1). Based on the concentration of the target DNA in *Psy* dPCR assay (Supplementary Material 4, Table S1), the highest abundance was recorded at the site L6 ($(1.54 \pm 0.27) \times 10^6$ cp/L), while the lowest concentration was observed at the site L1 ($(6.23 \pm 2.77) \times 10^4$ cp/L) (Supplementary Material 1, Table S1). The one-way ANOVA test showed a statistically significant difference in abundances between sites ($p < 0.01$) (Supplementary material 1, Tables S6 and S7), suggesting variable distribution of *Psy* population across the DTD Hydrosystem. A comparison of the methodologies revealed an average proportional difference of 33.42 % in calculated *Psy* abundance between the *cts*-based identification and dPCR, as determined by the Bland-Altman analysis. *Psy* population sizes determined using the traditional plating method combined with *cts* identification (Fig. 4c) were higher than those obtained by dPCR in seven out of eight sites. However, at the site L6, where

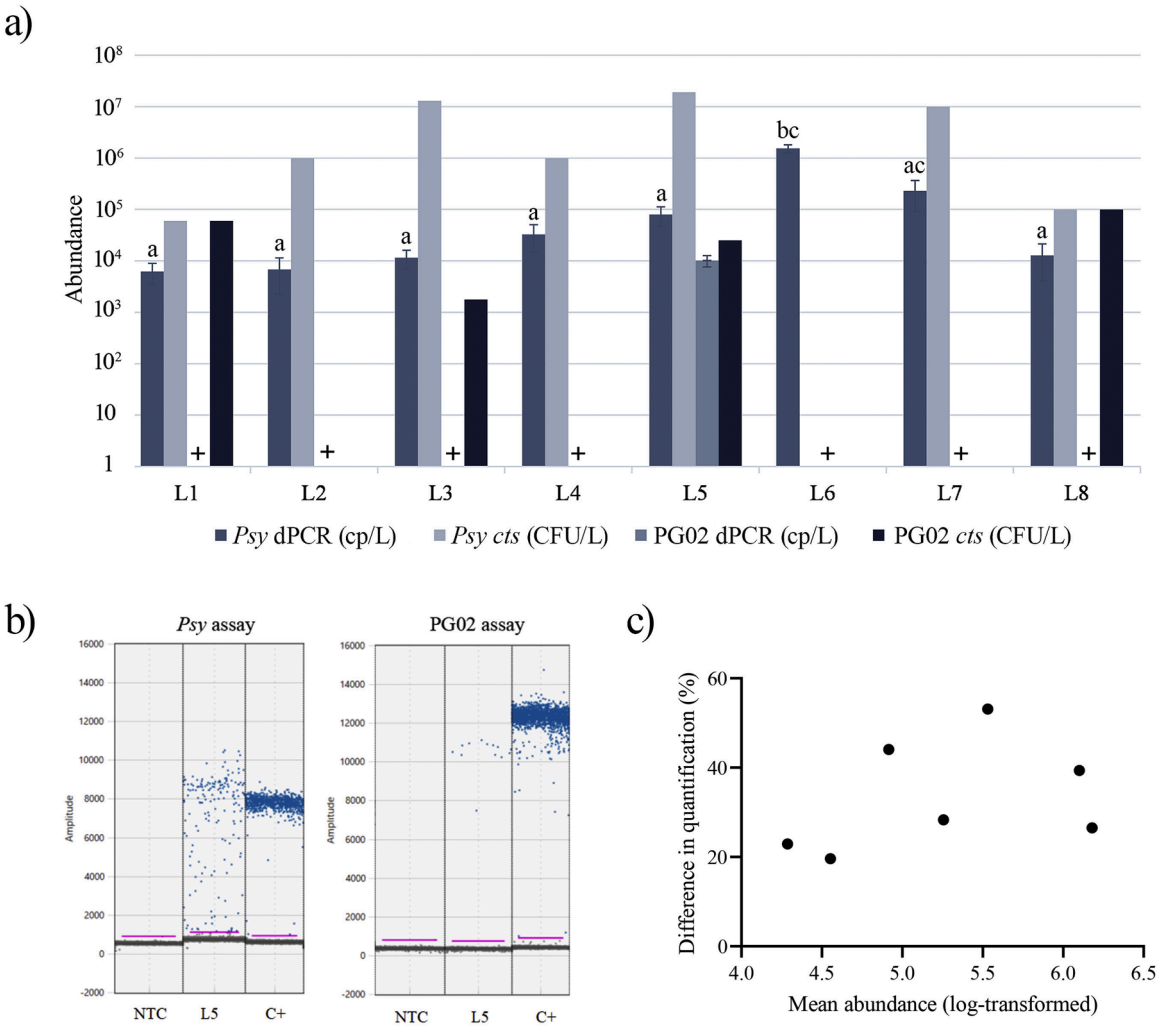

Fig. 4. The determined abundance of P. syringae complex and phylogroup 2 in the Danube-Tisa-Danube Hydrosystem assessed by dPCR and cts-based identification. a) Psy and PG02 abundances determined by both methods, presented on a logarithmic scale. Sites sharing the same letters (a, b, c) indicate no statistically significant differences in Psy abundance among these locations. PG02 was quantified by dPCR only at L5; at other sites, detection was below the quantification limit and is therefore interpreted qualitatively ('+' indicates the presence of PG02 at a given locality). b) Representative dPCR results of Psy and PG02 assays for site Bač (L5). Blue droplets indicate positive results, while grey droplets indicate negative results. NTC – no template control, *C*+ – positive control strain BFD143. c) Results of the Bland-Altman analysis showing the percentage difference in the quantification of Psy complex abundance between the cts-based identification and dPCR method.

Psy could not be successfully isolated using the plating method, dPCR successfully quantified its abundance, confirming the sensitivity and effectiveness of the method.

For PG02, at the site L5 concentration of the target DNA was above LOQ (Fig. 4 and Supplementary Material 4, Fig. S2). The determined abundance for site L5 based on dPCR results was $(1.01 \pm 0.25) \times 10^4$ cp/L. At other sites, the concentration of target DNA was below LOQ, but above the determined LOB (Supplementary Material 4, Table S2), thus confirming the presence of PG02. Site L5 is therefore the only location where PG02 was both detected and quantified by dPCR. At this site, six strains belonging to PG02 were isolated. Although PG02 strains were also isolated from sites L1, L3, and L8, the combination of the highly specific Psy_AvrE1 primer set and the sensitivity of dPCR enabled PG02 detection even at sites where no isolates were obtained. This underscores the limitations of cultivation-based methods that rely on a small number of isolates, as some groups may be missed. In contrast, dPCR demonstrates superior sensitivity for detecting low-abundance groups such as PG02.

4. Discussion

Despite extensive studies of the *Psy* complex in non-agricultural contexts (Morris et al., 2023), its routine monitoring in water habitats and irrigation sources remains largely overlooked. Yet, these environments often host highly diverse populations and include key pathogenic strains (Morris et al., 2010, 2013). Our study specifically examined the *Psy* complex in the DTD, a multipurpose irrigation network of substantial economic importance to Serbia (Milanović et al., 2011), therefore a valuable target for investigating the *Psy* population in aquatic environments.

One objective of our study was to develop, validate, and optimize qPCR and dPCR assays for detecting the *Psy* complex in water samples, as molecular methods are more reliable and widely used for pathogen detection (Venbrux et al., 2023). Since the target sequences used for detection are present as single copies, we also utilized this approach to estimate bacterial abundances. This method significantly accelerates the process by bypassing cultivation and molecular identification, thus enabling more feasible and efficient regular monitoring. Compared to qPCR, dPCR demonstrated superior performance in quantification, probably due to its lower susceptibility to inhibition, enhanced analytical sensitivity, reduced variability at the detection limit, and greater precision (Tiwari et al., 2022). Unlike qPCR, which only offers relative quantification, dPCR also enables absolute quantification (Kokkoris et al., 2021). Interestingly, abundance estimated by dPCR was the highest at the site where cultivation-based isolation failed. The lack of highly selective media likely reduces isolation recovery rates and may cause underestimation of the *Psy* abundance and diversity by allowing competition from non-target strains and bias against certain *Psy* strains, as observed with KBC media (Morris et al., 2008). Increasing the number of replicate plates could provide more accurate abundance estimates, though this approach is even more time-intensive and may not be convenient for rapid diagnostics.

For PG02, although the detection with the highly specific Psy_AvrE1 primer-probe set was successful, low target DNA concentrations likely influenced and limited quantification. The common practice of diluting the sample to mitigate the adverse effects of co-extracted inhibitors, such as trace amounts of organic acids, salts, metals, household detergents, pharmaceuticals, and personal care products (Venbrux et al., 2023) may also reduce trace target DNA concentrations in environmental samples (Shi et al., 2021). Working with eDNA at low target concentrations can lead to uneven distribution across replicate reactions, a technical challenge that affects the accuracy and reproducibility of assays.

Regarding the diversity of *Psy* in the DTD, while PG02, PG07, and PG13 were previously detected along the Danube River in Serbia (Anteljević et al., 2023), this study marks the first detection of PG01 and PG12 in Serbian water systems. Phylogroup 1 includes strains isolated from both diseased plants and environmental habitats, grouped into clades 1a and 1b (Berge et al., 2014). The PG07 strains we obtained belong to clade 7a and are identified as *P. viridiflava*, a species commonly found in various environmental sources (Lipps and Samac, 2022). In Serbia, *P. viridiflava* was identified as a causative agent of pit necrosis in tomato plants, in the southern part of the country (Popović et al., 2015c). Strains among the PG12 and PG13 are not considered pathogenic, and both groups are commonly found in irrigation water, but PG13 strains have also been isolated from asymptomatic plants (Berge et al., 2014).

Phylogroup 2 stands out as the most widely distributed within the *Psy* complex, comprising representatives from diseased plants, asymptomatic plants, and non-plant substrates (Berge et al., 2014). In the area surrounding the DTD canal network, most epidemics in the last years have been caused by representatives of this phylogroup (Fig. 1 and Supplementary Material 1, Table S2). The most vulnerable plant species included sugar beet, oil pumpkin, pea, carrot, parsley, parsnip, and sweet cherry (Balaž et al., 2014; Iličić et al., 2021; Popović et al., 2015a, 2015b; Stojšin et al., 2015). A broad host range of PG02 representatives has been demonstrated in nature and previous studies, with symptoms observed in over 75 % of tested plant species (Morris et al., 2019).

Epidemics on sugar beet, reported 10 years ago in Vojvodina (Stojšin et al., 2015; Nikolić et al., 2018) were attributed to the same haplotype now persisting in the DTD that matches *P. syringae* pv. *aptata* (Fig. 1). This haplotype, designated as DD.1, was reported as dominant in the Durance River catchment (Morris et al., 2023) and detected in river headwaters across the U.S., Europe, and New Zealand (Morris et al., 2010), and it has also been found in various plant-related contexts across four continents, which underscores its long-distance dissemination and potential for global spread (Morris et al., 2023). Its pathogenic potential is also notable, as we observed two groups of strains with differing levels of aggressiveness in our host range test, with the more aggressive group comprising isolates from the DD.1 haplotype (and others that differ by a single nucleotide from DD.1 in the *cts* gene sequence). The encounter location of highly aggressive strains aligns with nearby reported epidemic sites. In contrast, less aggressive strains were isolated from non-epidemic regions, suggesting a link between prior epidemics and the *Psy* population in the DTD. Specifically, the area around site L3 could be an important site for monitoring, as this part of the DTD harbors strains with a wide host range, capable of inducing severe symptoms in susceptible hosts, and closely related to the DD.1 haplotype, which was previously isolated from surrounding epidemics. However, no segment of the DTD should be neglected, as these strains could spread throughout the network and negatively affect a wide range of plants through irrigation.

As a leaf pathogen, *Psy* can effectively spread through sprinkling irrigation, which is the most commonly used method in Serbia (Statistical Office of the Republic of Serbia, 2024). A study demonstrated that an inoculum concentration as low as 1×10^2 CFU/mL is sufficient to induce characteristic midrib rot symptoms on lettuce when applied through overhead sprinkler irrigation (Cottyn et al., 2011). This finding highlights the pathogen's low threshold for initiating infection under favorable conditions, suggesting that some DTD sites may pose a significant threat to susceptible crops.

Understanding how *Psy* populations respond to nutrient-rich and microbially contaminated waters, such as those in the DTD system, requires further investigation and ongoing monitoring. A recent study on the Durance River catchment identified temperature as the primary factor influencing *Psy* abundance (Morris et al., 2023), but to our knowledge, the impact of organic pollutants on *Psy* populations has not been documented before.

5. Conclusions

Monitoring *Psy* populations in water systems connected to

agricultural fields is essential for assessing potential disease risks to crops. The *Psy* complex in the DTD demonstrated high strain diversity and significant pathogenic potential, which displayed a broad host range and the capacity for widespread dissemination, as evidenced by globally distributed haplotypes. In this study, we designed highly specific qPCR tests for the detection of PG02 of the *Psy* species complex. Also, we successfully utilized dPCR to detect and quantify *Psy* complex populations in irrigation water. At specific sites, *Psy* populations are abundant enough to trigger disease in susceptible hosts under favorable conditions, potentially highlighting the risk of extensive epidemics. Despite our efforts to quantify PG02 populations, low target concentrations restricted our results to qualitative analyses, emphasizing the need for improved sensitivity and specificity in detection methods. Enhanced monitoring strategies are crucial for the timely identification and management of *Psy* populations in irrigation systems to mitigate risks to crop health and agricultural productivity. Future studies should focus on refining molecular techniques and exploring the ecological dynamics of *Psy* in water systems to develop more effective disease prevention strategies.

CRediT authorship contribution statement

Marina Anteljević: Writing – original draft, Visualization, Validation, Methodology, Investigation, Formal analysis, Data curation, Conceptualization. **Iva Rosić:** Validation, Methodology, Investigation, Data curation, Conceptualization. **Olja Medić:** Writing – review & editing, Conceptualization. **Tamara Ranković:** Writing – review & editing, Conceptualization. **Karolina Sunjog:** Writing – review & editing, Investigation, Data curation. **Margareta Kračun-Kolarević:** Writing – review & editing, Investigation, Formal analysis. **Stoimir Kolarević:** Writing – review & editing, Visualization, Validation, Investigation, Formal analysis. **Tanja Dreo:** Supervision, Resources, Project administration, Conceptualization. **Aleksander Benčič:** Writing – review & editing, Validation, Investigation. **Tanja Berić:** Writing – review & editing, Conceptualization. **Slaviša Stanković:** Writing – review & editing, Supervision, Resources. **Ivan Nikolić:** Writing – review & editing, Validation, Supervision, Resources, Project administration, Methodology, Conceptualization.

Declaration of competing interest

The authors declare that they have no known competing financial interests or personal relationships that could have appeared to influence the work reported in this paper.

Acknowledgements

We would like to thank Mojca Milavec for her valuable contribution to establishing and supporting the collaboration that enabled this research. The content of this study is in line with following United Nations (UN) Sustainable Development Goals, under the frame of the UN Agenda for Sustainable Development (Transforming our World: The 2030 Agenda for Sustainable Development – UN, 2015): Goal 2: Zero hunger; Goal 6: Clean water and sanitation.

Funding

This work was supported by the Ministry of Science, Technological Development and Innovations of the Republic of Serbia, grants no 451-03-136/2025-03/200178, 451-03-137/2025-03/200178 (Faculty of Biology), 451-03-136/2025-03/200053 (Institute for Multidisciplinary Research), 451-03-136/2025-03/200007 (Institute for Biological Research 'Siniša Stanković' National Institute of the Republic of Serbia, University of Belgrade) and bilateral collaboration project between Serbia (Faculty of Biology, University of Belgrade) and Slovenia (National Institute of Biology), grant no 337-00-110/2023-05/47. The authors also acknowledge funding provided by the Institute of Physics, National Institute of the Republic of Serbia, through a grant by the Ministry of Science, Technological Development and Innovation of the Republic of Serbia.

Supplementary materials

Supplementary material associated with this article can be found, in the online version, at doi:10.1016/j.wroa.2025.100380.

Data availability

Data will be made available on request

References

Anteljević, M., Rosić, I., Medić, O., Kolarević, S., Berić, T., Stanković, S., Nikolić, I., 2023. Occurrence of plant pathogenic *Pseudomonas syringae* in the Danube River Basin: abundance and diversity assessment. Phytopathol. Res. 5 (1), 18. https://doi.org/10.1186/s42483-023-00174-0.

Balaž, J., Iličić, R., Maširević, S., Jošić, D., Kojić, S., 2014. First report of *Pseudomonas syringae* pv. *syringae* causing bacterial leaf spots of oil pumpkin (*Cucurbita pepo*) in Serbia. Plant Dis. 98 (5), 684. https://doi.org/10.1094/PDIS-07-13-0714-PDN.

Balthazar, C., Novinscak, A., Cantin, G., Joly, D.L., Filion, M., 2022. Biocontrol activity of *Bacillus* spp. And *Pseudomonas* spp. Against *botrytis cinerea* and other *cannabis* fungal pathogens. Phytopathology 112 (3), 549–560. https://doi.org/10.1094/PHYTO-03-21-0128-R.

Barrett-Manako, K., Andersen, M., Martínez-Sánchez, M., Jenkins, H., Hunter, S., Reese-George, J., Montefiori, M., Wohlers, M., Rikkerink, E., Templeton, M., Nardozza, S., 2021. Real-time PCR and droplet digital PCR are accurate and reliable methods to quantify *Pseudomonas syringae* pv. *actinidiae* biovar 3 in kiwifruit infected plantlets. Plant Dis. 105 (6), 1748–1757. https://doi.org/10.1094/PDIS-08-20-1703-RE.

Berge, O., Monteil, C.L., Bartoli, C., Chandeysson, C., Guilbaud, C., Sands, D.C., Morris, C.E., 2014. A user's guide to a data base of the diversity of *Pseudomonas syringae* and its application to classifying strains in this phylogenetic complex. PLoS ONE 9 (9), e105547. https://doi.org/10.1371/journal.pone.0105547.

Berge, O., Nofal, S., Razan, F., Chandeysson, C., Guilbaud, C., 2023. Groundwater as a reservoir for plant pathogenic bacteria : the case of *Pseudomonas syringae* Complex in the alluvial aquifer of Avignon. Preprints. https://doi.org/10.20944/preprints202306.0217.v1.

Blagojević, B., Langović, M., Novković, I., Dragićević, S., Živković, N., 2020. Introduction to water resources management in Balkan countries. In: Zelenakova, M., Negm, A. M., Minea, I. (Eds.), Water Resources Management in Balkan Countries, pp. 123–247. https://doi.org/10.1007/978-3-030-22468-4_1.

Chai, A.L., Ben, H.Y., Guo, W.T., Shi, Y.X., Xie, X.W., Li, L., Li, B.J., 2020. Quantification of viable cells of *Pseudomonas syringae* pv. *tomato* in tomato seed using propidium monoazide and a real-time PCR assay. Plant Dis. 104 (8), 2225–2232. https://doi.org/10.1094/PDIS-11-19-2397-RE.

Cheng, T.L., Liao, C.C., Tsai, W.H., Lin, C.C., Yeh, C.W., Teng, C.F., Chang, W.T., 2009. Identification and characterization of the mitochondrial targeting sequence and mechanism in human citrate synthase. J. Cell. Biochem. 107 (5), 1002–1015. https://doi.org/10.1002/jcb.22200.

Clinical and Laboratory Standards Institute, 2004. Protocols For Determination of Limits of Detection and Limits of quantitation: Approved guideline (NCCLS Document EP17-A (ISBN 1-56238-551-8).

Corona-López, E., Román-Gutiérrez, A.D., Otazo-Sánchez, E.M., Guzmán-Ortiz, F.A., Acevedo-Sandoval, O.A., 2021. Water–Food Nexus assessment in agriculture: a systematic review. Int. J. Environ. Res. Public Health. 18 (9), 4983. https://doi.org/10.3390/ijerph18094983.

Cottyn, B., Baeyen, S., Pauwelyn, E., Verbaendert, I., De Vos, P., Bleyaert, P., Hofte, M., Maes, M., 2011. Development of a real-time PCR assay for *Pseudomonas cichorii*, the causal agent of midrib rot in greenhouse-grown lettuce, and its detection in irrigating water. Plant Pathol 60 (3), 453–461. https://doi.org/10.1111/j.1365-3059.2010.02388.x.

de Araujo, G.G., Rodrigues, F., Gonçalves, F.L.T., Galante, D., 2019. Survival and ice nucleation activity of *Pseudomonas syring*ae strains exposed to simulated high-altitude atmospheric conditions. Sci. Rep. 9 (1), 1–11. https://doi.org/10.1038/s41598-019-44283-3.

Dinno, A., 2017. dunn. Test: dunn's test of multiple comparisons using rank sums. R package version 1 (5), 1. https://cran.r-project.org/package=dunn.test.

FAO, 2022. FAOSTAT: Crops and livestock products. Accessed on November 2, 2024. https://www.fao.org/faostat/en/#data/QCL.

FAO, 2021. Law on Agricultural Land, Official Gazette of the Republic of Serbia, No. 11/2021. FAOLEX database. Accessed on November 2, 2024. https://faolex.fao.org/docs/pdf/srb195486.pdf.

Guilbaud, C., Morris, C.E., Barakat, M., Ortet, P., Berge, O., 2016. Isolation and identification of *Pseudomonas syringae* facilitated by a PCR targeting the whole *P. syringae* group. FEMS Microbiol. Ecol. 92 (1), 1–9. https://doi.org/10.1093/femsec/fiv146.

Ignjatov, M., Milošević, D., Nikolić, Z., Gvozdanović-Varga, J., Tatić, M., Popović, T., Ivanović, Ž., 2017. The first report was that *fusarium tricinctum* causes rot in garlic

bulbs in Serbia. Plant Dis. 101 (2), 382. https://doi.org/10.1094/PDIS-09-16-1333-PDN.
Iličić, R., Balaž, J., Ognjanov, V., Popović Milovanović, T., 2021. Epidemiology studies of *Pseudomonas syringae* pathovars associated with bacterial canker on the sweet cherry in Serbia. Plant Protect. Sci. 57 (3), 196–205. https://doi.org/10.17221/140/2020-PPS.
Kokkoris, V., Vukicevich, E., Richards, A., Thomsen, C., Hart, M.M., 2021. Challenges using droplet digital PCR for environmental samples. Appl. Microbiol. 1 (1), 74–88. https://doi.org/10.3390/applmicrobiol1010007.
Krstić Tomić, T., Atanasković, I., Nikolić, I., Joković, N., Stević, T., Stanković, S., Berić, T., Lozo, J., 2023. Culture-dependent and metabarcoding characterization of the sugar beet (*Beta vulgaris* L.) microbiome for high-yield isolation of bacteria with plant growth-promoting traits. Microorganisms 11 (6), 1538. https://doi.org/10.3390/microorganisms11061538.
Lamichhane, J.R., Bartoli, C., 2015. Plant pathogenic bacteria in open irrigation systems: what risk for crop health? Plant Pathol 64 (4), 757–766. https://doi.org/10.1111/ppa.12371.
Letunic, I., Bork, P., 2024. Interactive Tree of Life (iTOL) v6: recent updates to the phylogenetic tree display and annotation tool. Nucl. Acid. Res. 52 (W1), W78–W82. https://doi.org/10.1093/nar/gkae268.
Lipps, S.M., Samac, D.A., 2022. *Pseudomonas viridiflava*: an internal outsider of the *Pseudomonas syringae* species complex. Mol. Plant Pathol. 23 (1), 3–15. https://doi.org/10.1111/mpp.13133.
Marković, S., Milić Komić, S., Jelušić, A., Iličić, R., Bagi, F., Stanković, S., Popović, T., 2022. First report of *pectobacterium versatile* causing blackleg of potato in Serbia. Plant Dis. 106 (1), 312. https://doi.org/10.1094/PDIS-06-21-1128-PDN.
Meier-Kolthoff, J.P., Göker, M., 2019. TYGS is an automated high-throughput platform for state-of-the-art genome-based taxonomy. Nat. Commun. 10 (1), 2182. https://doi.org/10.1038/s41467-019-10210-3.
Milanović, A., Milijašević, D., Brankov, J., 2011. Assessment of polluting effects and surface water quality using water pollution index: a case study of Hydro–system Danube–Tisa–Danube, Serbia. Carpath. J. Earth Environ. Sci. 6 (2), 269–277.
Mitrović, M., Cvrković, T., Jović, J., Krstić, O., Jakovljević, M., Kosovac, A., Toševski, I., 2015. First report of 'candidatus *phytoplasma solani* 'Infecting garden bean *phaseolus vulgaris* in Serbia. Plant Dis. 99 (4), 551. https://doi.org/10.1094/PDIS-10-14-1052-PDN.
Mohan, S.K., 1987. An improved agar plating assay for detecting *Pseudomonas syringae* pv. *syringae* and *P. s.* pv. *phaseolicola* in contaminated bean seed. Phytopathology 77 (10), 1390. https://doi.org/10.1094/phyto-77-1390.
Morris, C.E., Lacroix, C., Chandeysson, C., Guilbaud, C., Monteil, C., Piry, S., Rochelle Newall, E., Fiorini, S., Van Gijsegem, F., Barny, M.A., Berge, O., 2023. Comparative abundance and diversity of populations of the *Pseudomonas syringae* and Soft Rot *Pectobacteriaceae* species complexes throughout the Durance River catchment from its French Alps sources to its delta. Peer Commun. J. 3, e88, 10.24072/pcjournal.317.
Morris, C.E., Lamichhane, J.R., Nikolić, I., Stanković, S., Moury, B., 2019. The overlapping continuum of host range among strains in the *Pseudomonas syringae* complex. Phytopathol. Res. 1 (1), 1–16. https://doi.org/10.1186/s42483-018-0010-6.
Morris, C.E., Monteil, C.L., Berge, O., 2013. The life history of *Pseudomonas syringae*: linking agriculture to earth system processes. Annu. Rev. Phytopathol. 51, 85–104. https://doi.org/10.1146/annurev-phyto-082712-102402.
Morris, C.E., Ramirez, N., Berge, O., Lacroix, C., Monteil, C., Chandeysson, C., Guilbaud, C., Blischke, A., Sigurbjörnsdóttir, M.A., Vilhelmsson, O., 2022. *Pseudomonas syringae* on plants in Iceland has likely evolved for several million years outside the reach of processes that mix this bacterial complex across earth's temperate zones. Pathogens 11 (3), 357. https://doi.org/10.3390/pathogens11030357.
Morris, C.E., Sands, D.C., Vanneste, J.L., Montarry, J., Oakley, B., Guilbaud, C., Glaux, C., 2010. Inferring the evolutionary history of the plant pathogen *Pseudomonas syringae* from its biogeography in headwaters of rivers in North America, Europe, and New Zealand. MBio 1 (3), e00107–e00110. https://doi.org/10.1128/mBio.00107-10.
Morris, C.E., Sands, D.C., Vinatzer, B.A., Glaux, C., Guilbaud, C., Buffiere, A., Thompson, B.M., 2008. The life history of the plant pathogen *Pseudomonas syringae* is linked to the water cycle. ISME J. 2 (3), 321–334. https://doi.org/10.1038/ismej.2007.113.
Nikolić, I., Stanković, S., Dimkić, I., Berić, T., Stojšin, V., Janse, J., Popović, T., 2018. Genetic diversity and pathogenicity of *Pseudomonas syringae* pv. *aptata* isolated from sugar beet. Plant. Pathol. 67 (5), 1194–1207. https://doi.org/10.1111/ppa.12831.
Official Gazette of the Republic of Serbia No.74/2011 (2011). Regulation on the parameters of ecological and chemical status of surface water and parameters of the chemical and quantitative status of groundwater.
Pirc, M., Ravnikar, M., Tomlinson, J., Dreo, T., 2009. Improved fireblight diagnostics using quantitative real-time PCR detection of *Erwinia amylovora* chromosomal DNA. Plant Pathol. 58 (5), 872–881. https://doi.org/10.1111/j.1365-3059.2009.02083.x.
Popović, T., Balaž, J., Starović, M., Trkulja, N., Ivanović, Ž., Ignjatov, M., Jošić, D., 2013. First report of *Xanthomonas campestris* pv. *campestris* as the causal agent of black rot on oilseed rape (*Brassica napus*) in Serbia. Plant Dis. 97 (3), 418. https://doi.org/10.1094/PDIS-05-12-0506-PDN.
Popović, T., Ivanović, Ignjatov, M., 2015c. First report of *Pseudomonas viridiflava* causing pith necrosis of tomato (*Solanum lycopersicum*) in Serbia. Plant Dis. 99 (7), 1033. https://doi.org/10.1094/PDIS-01-15-0052-PDN.
Popović, T., Ivanović, Ž., Ignjatov, M., Milošević, D., 2015a. First report of *Pseudomonas syringae* pv. *coriandricola* causing bacterial leaf spot on carrot, parsley and parsnip in Serbia. Plant Dis. 99 (3), 416. https://doi.org/10.1094/PDIS-10-14-1041-PDN.
Popović, T., Ivanović, Ž., Trkulja, N., Milosavljević, A., Ignjatov, M., 2015b. First report of *Pseudomonas syringae* pv. *syringae* on pea (*Pisum sativum*) in Serbia. Plant Dis. 99 (5), 724. https://doi.org/10.1094/PDIS-11-14-1212-PDN.
R Core Team, 2024. R: a language and environment for statistical computing. R Foundation for Statistical Computing, Vienna, Austria. https://www.Rproject.org/.
Salem, H.S., Pudza, M.Y., Yihdego, Y., 2022. Water strategies and water–food nexus: challenges and opportunities towards sustainable development in various regions of the World. Sustain. Water Resour. Manag. 8 (4), 114. https://doi.org/10.1007/s40899-022-00676-3.
Schneider, C.A., Rasband, W.S., Eliceiri, K.W., 2012. NIH image to ImageJ: 25 years of image analysis. Nat. Method. 9 (7), 671–675. https://doi.org/10.1038/nmeth.2089.
Shi, X., Liu, G., Shi, L., Chen, M., Wu, X., Lu, Y., Zhao, J., 2021. The detection efficiency of digital PCR for the virulence genes of waterborne pathogenic bacteria. Water Supply 21 (5), 2285–2297. https://doi.org/10.2166/ws.2021.056.
Statistical Office of the Republic of Serbia, 2024. Monthly statistical bulletin: February 2024. Accessed on November 2, 2024. https://publikacije.stat.gov.rs/G2024/Pdf/G20242057.pdf.
Stojšin, V., Balaž, J., Budakov, D., Stanković, S., Nikolić, I., Ivanović, Ž., Popović, T., 2015. First report of *Pseudomonas syringae* pv. *aptata* causing bacterial leaf spot on sugar beet in Serbia. Plant Dis. 99 (2), 281. https://doi.org/10.1094/PDIS-06-14-0628-PDN.
Tiwari, A., Ahmed, W., Oikarinen, S., Sherchan, S.P., Heikinheimo, A., Jiang, G., Simpson, S.L., Greaves, J., Bivins, A., 2022. Application of digital PCR for public health-related water quality monitoring. Sci. Total Environ. 837, 155663. https://doi.org/10.1016/j.scitotenv.2022.155663.
Thomsen, M.C.F., Hasman, H., Westh, H., Kaya, H., Lund, O., 2017. RUCS: rapid identification of PCR primers for unique core sequences. Bioinformatics 33 (24), 3917–3921. https://doi.org/10.1093/bioinformatics/btx526.
Venbrux, M., Crauwels, S., Rediers, H., 2023. Current and emerging trends in techniques for plant pathogen detection. Front. Plant Sci. 14, 1–25. https://doi.org/10.3389/fpls.2023.1120968.
Wickham, H., 2016. Data analysis. Title of the Book. Springer International Publishing, pp. 189–201. https://doi.org/10.1007/978-3-319-24277-4_9.
Yang, P., Zhao, L., Gao, Y.G., Xia, Y., 2023. Detection, diagnosis, and preventive management of the bacterial plant pathogen *Pseudomonas syringae*. Plants 12 (9), 1765. https://doi.org/10.3390/plants12091765.